PHYSICAL REVIEW B **89**, 045133 (2014)

Conducting fixed points for inhomogeneous quantum wires: A conformally invariant boundary theory

N. Sedlmayr,[1,*] D. Morath,[1] J. Sirker,[1] S. Eggert,[1] and I. Affleck[2]

[1]*Department of Physics and Research Center OPTIMAS, University of Kaiserslautern, D-67663 Kaiserslautern, Germany*

[2]*Department of Physics and Astronomy, The University of British Columbia, Vancouver, British Colombia, Canada, V6T 1Z1*

(Received 29 October 2013; published 24 January 2014)

Inhomogeneities and junctions in wires are natural sources of scattering, and hence resistance. A conducting fixed point usually requires an adiabatically smooth system. One notable exception is "healing," which has been predicted in systems with special symmetries, where the system is driven to the homogeneous fixed point. Here we present theoretical results for a different type of conducting fixed point which occurs in inhomogeneous wires with an abrupt jump in hopping and interaction strength. We show that it is always possible to tune the system to an unstable conducting fixed point which does not correspond to translational invariance. We analyze the temperature scaling of correlation functions at and near this fixed point and show that two distinct boundary exponents appear, which correspond to different effective Luttinger liquid parameters. Even though the system consists of two separate interacting parts, the fixed point is described by a single conformally invariant boundary theory. We present details of the general effective bosonic field theory including the mode expansion and the finite size spectrum. The results are confirmed by numerical quantum Monte Carlo simulations on spinless fermions. We predict characteristic experimental signatures of the local density of states near junctions.

DOI: 10.1103/PhysRevB.89.045133 PACS number(s): 73.63.Nm, 71.10.Pm, 73.40.−c

I. INTRODUCTION

Transport in quantum wires is a rich field bringing together conductivity experiments [1–5] and Luttinger liquid theory which describes the crucial electron-electron interaction effects in one dimension [6–8]. Scattering from a single impurity or other inhomogeneities, for example, becomes renormalized by the interaction and can lead to insulating behavior at low temperatures even for weak impurities [9–14].

To determine the conductivity of a one-dimensional wire it is necessary to couple it to some leads or reservoirs, normally a two-dimensional electron gas (2DEG). Such a setup can be most readily described as an inhomogeneous wire, in which the 2DEGs are modeled as noninteracting wires. In this case the conductance is usually controlled by the parameters of the lead rather than of the wire [15–28], in contrast to what a naive calculation on an *infinite* interacting wire would suggest. The conductance for perfect adiabatic contacts and wires can be understood by the decomposition of an electron into fractional charges [16,29]. Additional relaxation processes which take place within the interacting region of the wire do, however, lead to a resistance which is affected by the wire parameters. The resistance due to impurity scattering [30] or phonon scattering [28] within the interacting wire, for example, will in general depend both on the Luttinger liquid parameter of the leads and the wire.

In this paper we consider the intrinsic scattering from the junctions between the wire and leads, which is generically present due to the abrupt change of parameters even for otherwise perfect ballistic connections. This scattering is renormalized by the interaction [30], leading to a vanishing dc conductance in the low temperature limit for repulsive interactions within the wire. However, perfect conductance is still possible by tuning the parameters on the two sides of the junctions as has been analyzed in detail for a particle-hole symmetric model [27]. In this case a line of conducting fixed points in parameter space exists as only one relevant backscattering operator is permitted by symmetry which can always be tuned to zero. Here we generalize to the more experimentally relevant case where particle-hole symmetry is no longer present. Even in this more general case we still find a line of conducting fixed points provided the underlying microscopic theory has certain local symmetry properties. Even though the systems under consideration are inhomogeneous, it is possible to characterize the fixed points by a single conformally invariant boundary theory with a characteristic mode expansion and finite size spectrum. The results are confirmed by numerical quantum Monte Carlo (QMC) simulations on spinless fermions. Characteristic experimental signatures for the local density of states near junctions can be predicted.

For conductivity experiments we must typically consider a system with two junctions, one at each end of an interacting wire where it is connected to the leads (e.g., 2DEGs). These junctions are intrinsic sources of inhomogeneity, but in most cases the junctions do not influence each other since the length of the wire is much larger than the coherence length $u\beta$, where β is the inverse temperature and u the velocity of the collective excitations. For our purpose to make predictions for the backscattering and the local behavior near the leads, it is therefore sufficient to analyze one junction between a lead and a wire.

As an introduction in Sec. II we consider an idealized junction in a noninteracting lattice model and discuss the applicability of a narrow band approximation. In Sec. III we start from a microscopic interacting model and demonstrate how the backscattering terms arise, and then introduce the general effective bosonic field theory. Focusing on abrupt junctions connecting otherwise homogeneous wires, we examine the renormalization group flow of perturbing operators in the model. We discuss the locations of the unstable conducting

*nicholas.sedlmayr@cea.fr

fixed points in relation to the symmetry properties of the underlying microscopic model. Finally in Sec. IV we describe the conformally invariant boundary theory for the conducting fixed point and the scaling of the local correlation functions at the boundary. In Sec. V we conclude.

II. NONINTERACTING MODELS

Before considering the interacting model it is instructive to analyze the backscattering seen in inhomogeneous systems of free particles, where exact results are obtainable and can be compared directly with low energy approximations. We start with a lattice model of noninteracting spinless fermions described by the Hamiltonian

$$\hat{H}_0 - \mu N = -\sum_j [t_j(\psi_j^\dagger \psi_{j+1} + \text{H.c.}) - V_j \psi_j^\dagger \psi_j]. \quad (2.1)$$

$\psi_j^\dagger$ creates a particle at site j, t_j and V_j are the position-dependent hopping elements and local potential energy respectively, and N the total particle number. We set $\hbar = 1$ and include in the following the chemical potential μ in the local potential energy V_j. Generically we consider situations in which we have two homogeneous regions on the left ($j \leqslant j_\ell$) and right ($j \geqslant j_r$) sides of the wire. In these asymptotic regions the plane-wave solutions have the same energy so the parameters are related by

$$-2t_\ell \cos[k_\ell a] + V_\ell = -2t_r \cos[k_r a] + V_r, \quad (2.2)$$

with $k_{\ell,r}$ the momenta, $V_{\ell,r}$ the potential, and $t_{\ell,r}$ the hopping on the left (ℓ) and right (r) sides. We have also introduced the lattice spacing a. We consider a wave-function incident from the left

$$\psi_j = \begin{cases} e^{ik_\ell j} + Re^{-ik_\ell j}, & j \leqslant j_\ell, \\ Te^{ik_r j}, & j \geqslant j_r. \end{cases} \quad (2.3)$$

The region from j_ℓ to j_r is the region of inhomogeneity describing the junction.

There are two velocities

$$u_i \equiv 2at_i \sin[k_i a], \quad (2.4)$$

$i = \{\ell, r\}$, and the current conservation implies

$$(1 - |R|^2)u_\ell = |T|^2 u_r. \quad (2.5)$$

It is natural to refer to $R = 0$ as "perfect transmission," although this does not necessarily maximize $|T|^2$. A reasonable definition of perfect transmission would be maximizing the outgoing current on the right for a given value of the incoming current from the left u_ℓ; that is, maximizing $|T|^2 u_r/u_\ell$. Noting that $|T|^2 u_r/u_\ell = 1 - |R|^2$ we see that the condition for perfect transmission equivalently corresponds to minimizing $|R|^2$. This can also be seen by considering the Landauer transmission, see Appendix A.

In general, accurate results cannot be obtained by ignoring states far from the Fermi energy. This can be seen from the fact that the off-diagonal components of the T matrix, $T_{k,k'}$, are nonnegligible when $|k'|$ is not close to $|k|$. This implies a nonnegligible mixing of low energy states with high energy ones due to scattering near the interface. However, in certain limits, a narrow band theory can be used, in which we keep only a narrow band of states, of width $\Lambda \ll k_F$, where k_F is the Fermi momentum, and linearize the dispersion relation. This can be justified in one of two cases. (a) If all potential energy terms V_i and all hopping terms t_i are nearly equal, including the asymptotic ones $t_\ell \approx t_r$. This corresponds to the adiabatic limit where a local density approximation suffices. (b) If there are one or more very weak hopping terms separating otherwise uniform chains. In this latter case the ratio t_ℓ/t_r can be arbitrary. These are the limits of weak backscattering or weak tunneling. Starting with the unperturbed basis of translationally invariant wave functions, or wave functions vanishing at the interface, respectively, a small perturbation only mixes states with energy differences of the order of magnitude of the perturbation.

In these cases we may keep only a narrow band of states near zero energy and introduce left and right moving fields in the usual way,

$$\frac{\psi_j}{\sqrt{a}} \approx e^{ik_{F,x}x}\psi_+(x) + e^{-ik_{F,x}x}\psi_-(x), \quad (2.6)$$

with $x = aj$ a continuous variable and k_{Fx} being the Fermi momentum in the left, $k_{F,x\leqslant aj_\ell} = k_{F\ell}$, or right, $k_{F,x\geqslant aj_r} = k_{Fr}$, of the wire.

Here we want to consider only the simplest model for a junction while various other types of junctions are discussed in Appendix B. In the simplest model two homogeneous regions are connected at one site such that

$$t_j = \begin{cases} t_\ell, & j < 0, \\ t_r, & j \geqslant 0, \end{cases} \qquad V_i = \begin{cases} V_\ell, & j < 0, \\ V_r, & j > 0, \end{cases} \quad (2.7)$$

and V_0 is kept as a free parameter. The reflection amplitude is determined by the Schrödinger equation for the central site and results in

$$R = -\frac{a(V_\ell + V_r - 2V_0) - i(u_\ell - u_r)}{a(V_\ell + V_r - 2V_0) + i(u_\ell + u_r)}. \quad (2.8)$$

The conditions for perfect transmission are therefore

$$u_\ell = u_r, \text{ and} \qquad V_0 = (V_\ell + V_r)/2. \quad (2.9)$$

When these conditions are satisfied, $R = 0$ and $|T|^2 = 1$. Curiously, the maximum possible value of $|T|^2$ actually occurs when $V_0 = (V_\ell + V_r)/2$ and $u_r = 0$, in which case $|R| = 1$ and $|T| = 2$. But in this case the current is actually zero on both sides, so calling this perfect transmission would seem inappropriate. The existence of the two conditions (2.9) for perfect conductance is related to the breaking of particle-hole symmetry, see Sec. III A.

Next, we consider the abrupt junction of Eq. (2.7) in a narrow band approximation setting $t_\ell = t - \delta t$ and $t_r = t + \delta t$, with $|\delta t| \ll t$. When $\delta t = 0$ we obtain the usual free, translationally invariant Dirac fermion model, with uniform velocity $u_0 = 2at \sin k_F$. Here we treat the δt term as a

perturbation. Using the separation into right and left moving fields, Eq. (2.6), the backscattering at the junction is given by

$$\delta\hat{H} \approx -a\left[\sum_{j=-\infty}^{-1}(2t_\ell e^{ik_{F\ell}a}-V_\ell)e^{2ik_{F\ell}ja}+2t_r e^{ik_{Fr}a}\right.$$
$$\left.-\ V_0+\sum_{j=1}^{\infty}(2t_r e^{ik_{Fr}a}-V_r)e^{2ik_{Fr}ja}\right]\psi_-^\dagger\psi_+ + \text{H.c.} \quad (2.10)$$

Since $\psi_-(x)$ and $\psi_+(x)$ are assumed to vary slowly on the scale of $k_{F\ell/r}^{-1}$ the oscillating terms in the bulk cancel, leaving only the contributions at $x=0$. We may then write the local backscattering at $x=0$ as

$$\delta\hat{H} \approx 2\pi i\lambda\psi_-^\dagger\psi_+(x=0)+\text{H.c.} \quad (2.11)$$

with (see also Appendix E)

$$\begin{aligned}\text{Re}\,\lambda &= \frac{a}{2\pi}\left(\frac{t_\ell}{\sin[k_{F\ell}a]}-\frac{t_r}{\sin[k_{Fr}a]}\right)\\ &\quad -\frac{a}{4\pi}\left(V_\ell\cot[k_{F\ell}a]-V_r\cot[k_{Fr}a]\right)\\ &= \frac{a}{2\pi}\left(t_\ell\sin[k_{F\ell}a]-t_r\sin[k_{Fr}a]\right),\\ \text{Im}\,\lambda &= \frac{a}{4\pi}\left(V_\ell+V_r-2V_0\right),\end{aligned} \quad (2.12)$$

where we have used Eq. (2.2) to simplify the real part. We see that the scattering amplitude λ is real if the local potential energies are equal, $V_0=V_\ell=V_r$. This is surprising because for any nonzero local potential the problem is no longer particle-hole symmetric. In Appendix B we show that this is a special property of the junction (2.7) and does not hold in general. Finally, we can use the fact that we are treating the difference in hopping δt perturbatively and approximate $k_{F\ell}\approx k_{Fr}\approx k_F$ in which case the real part of the scattering amplitude further simplifies,

$$\text{Re}\,\lambda = -\frac{a\,\delta t}{\pi}\sin[k_F a]=\frac{u_\ell-u_r}{4\pi}, \quad (2.13)$$

where the difference in velocities on the two sides of the junction is given by $u_r-u_\ell=4a\delta t\sin[k_F a]$. We see that for $V_0\approx V_\ell\approx V_r$ and $u_\ell\approx u_r$, required for the narrow band approximation to be valid, the result for the scattering amplitude λ is fully consistent with the exact result for the reflection amplitude (2.8) by using the general relation $R=4\pi\lambda/(u_r+u_\ell)$ between these two quantities in this limit. In Sec. III A we will discuss how the narrow band calculation for this type of junction can be extended to the interacting case using bosonization.

III. INTERACTING MODEL

As a microscopic interacting model we use the Hamiltonian $\hat{H}=\hat{H}_0+\hat{H}_I$, where $\hat{H}_0$ is given by Eq. (2.1) and

$$\hat{H}_I=\sum_j U_j :\psi_j^\dagger\psi_j::\psi_{j+1}^\dagger\psi_{j+1}: \quad (3.1)$$

for interactions with a position-dependent nearest-neighbor interaction strength U_j. Normal ordered operators are given by $:\psi_j^\dagger\psi_j:=\psi_j^\dagger\psi_j-\langle 0|\psi_j^\dagger\psi_j|0\rangle$, with $|0\rangle$ the ground state. It is assumed that the spatial variation of U_j, t_j, and V_j in $\hat{H}_0$, is consistent with the narrow band approximation explained in the preceding section. Later we will focus on the limiting case of an abrupt jump in the interaction and hopping parameters at the junction, as used elsewhere [16,17,27,29,30].

To find the underlying low energy bosonic theory, we first need to linearize the spectrum. Analogously to the normal Luttinger liquid theory [6–8], one can linearize around the bulk band structure in the left and right regions of the wire [27]. Linearization is performed around the Fermi momenta $k_{F,x}$ for left and right movers:

$$\frac{\psi_j}{\sqrt{a}}=\psi(x)=\sum_{\alpha=\pm}e^{i\alpha k_{F,x}x}\psi_\alpha(x), \quad (3.2)$$

with the appropriate commutation relations $[\psi_\alpha(x),\psi_\beta(x')]_+=0$ and $[\psi_\alpha(x),\psi_\beta^\dagger(x')]_+=\delta_{\alpha\beta}\delta(x-x')$. Here $k_{F,x}$ is defined by $-2t\cos k_{F,x}+V_x=0$. Note that it is not necessary to assume that $k_{F\ell}\approx k_{Fr}$.

After linearization of the free Hamiltonian we find

$$\begin{aligned}\hat{H}_0 &= -\int dx\sum_{\alpha=\pm}at_x[e^{i\alpha\kappa_x^-}\psi_\alpha^\dagger(x)\partial_x\psi_\alpha(x)+\text{H.c.}]\\ &\quad -\int dx\sum_{\alpha=\pm}[2t_x e^{-2i\alpha\kappa_x^+}-V_x e^{-2i\alpha k_{F,x}}]\\ &\quad\times\psi_\alpha^\dagger(x)\psi_{-\alpha}(x),\end{aligned} \quad (3.3)$$

where the Fermi momenta are determined by

$$V_x=2t_x\cos[\kappa_x^-], \quad (3.4)$$

and we have defined $\kappa_x^-=k_{F,x+a}(x+a)-k_{F,x}x$ and $2\kappa_x^+=k_{F,x+a}(x+a)+k_{F,x}x$. Similarly, one can write the linearized interaction as

$$\begin{aligned}\hat{H}_I &= \sum_{\alpha,\beta=\pm}\int dx a U_x(:\psi_\alpha^\dagger\psi_\alpha(x)::\psi_\beta^\dagger\psi_\beta(x+a):\\ &\quad +e^{-\beta 2ik_{F,x+a}(x+a)}:\psi_\alpha^\dagger\psi_\alpha(x)::\psi_\beta^\dagger\psi_{-\beta}(x+a):\\ &\quad +e^{-\alpha 2ik_{F,x}x}:\psi_\alpha^\dagger\psi_{-\alpha}(x)::\psi_\beta^\dagger\psi_\beta(x+a):\\ &\quad +e^{-\alpha 2ik_{F,x}x-\beta 2ik_{F,x+a}(x+a)}\\ &\quad\times:\psi_\alpha^\dagger\psi_{-\alpha}(x)::\psi_\beta^\dagger\psi_{-\beta}(x+a):),\end{aligned} \quad (3.5)$$

keeping for the moment all of the terms. If the interaction acts homogeneously then many of the terms can be neglected as they are suppressed by the rapidly oscillating phases. Due to the inhomogeneity in U_x this is no longer true and all processes could in principle be important. In fact we find that umklapp scattering is generically irrelevant under renormalization group (RG) flow, see Appendix D, and to lowest order the backscattering only renormalizes the single particle backscattering already present in the noninteracting Hamiltonian.

We bosonize using the local vertex operator [31,32]

$$\psi_\alpha(x)=\frac{1}{\sqrt{2\pi a}}e^{i\alpha\sqrt{4\pi}[\phi_\alpha(x)]}. \quad (3.6)$$

We use the following convention: $\phi(x) = \phi_+(x) + \phi_-(x)$ and its adjoint $\tilde{\phi}(x) = \phi_+(x) - \phi_-(x)$ with the conjugate momentum, $\Pi(x) = \partial_x \tilde{\phi}(x)$. These fields obey

$$\begin{aligned}[\phi_+(x),\phi_-(y)] &= -\frac{i}{4},\\ [\phi_\alpha(x),\phi_\alpha(y)] &= \frac{i\alpha}{4}\,\mathrm{sgn}(y-x), \text{ and}\\ [\phi(x),\Pi(y)] &= i\delta(x-y)\,.\end{aligned} \tag{3.7}$$

Some further useful formulas for bosonization are given in Appendix C.

The full Hamiltonian $\hat{H} = \hat{H}_0 + \hat{H}_I$ can be rewritten in the bosonic representation as a quadratic Hamiltonian, a local backscatterer, and umklapp scattering: $\hat{H} = \hat{H}_b + \hat{H}' + \hat{H}_U$, see Appendix C for details. As already mentioned, away from half-filling the umklapp scattering term $\hat{H}_U$ becomes a local perturbation confined to the regions where U_j is varying, and is then irrelevant under RG flow. It is neglected in the following. We find the quadratic term to be

$$\hat{H}_b = \int dx \frac{u_x}{2}\left(\frac{1}{g_x}(\partial_x\phi)^2 + g_x(\partial_x\tilde{\phi})^2\right). \tag{3.8}$$

To lowest order we can determine the renormalized velocity

$$u_x \approx 2at_x \sin[\kappa_x^-]\left(1 + \frac{U_x}{\pi t_x}\sin[\kappa_x^-]\right), \tag{3.9}$$

and the Luttinger parameter

$$g_x \approx 1 - \frac{U_x}{\pi t_x}\sin[\kappa_x^-]\,. \tag{3.10}$$

The local backscattering from all processes in Eqs. (3.3) and (3.5) can be summarized in one term

$$\hat{H}' = \sum_{\substack{x=ja\\ j\in\mathbb{Z}}} \frac{1}{2\pi i} e^{-i\sqrt{4\pi}\phi(x) - 2ik_{F,x}x}\left[\frac{e^{-i\kappa_x^-}u_x}{a\sin[\kappa_x^-]} - V_x\right] + \text{H.c.} \tag{3.11}$$

We keep the sum over $x = ja$ here discrete to avoid ambiguity as to what the alternating terms are in the continuum limit. This also helps the precise calculation of these sums.

A. An abrupt junction

Let us now focus on the simple junction considered already in the previous section for the noninteracting case where two semi-infinite wires are joined at $x = 0$ with $t_{x<0} = t_\ell$, $t_{x\geqslant 0} = t_r$, and U_x defined equivalently. The local potential energy is taken to be uniform, $V_j = V$, except where explicitly said to the contrary. The Fermi momenta, $k_{F,x}$, can also be written with a similar structure as $k_{F,x<0} = k_{F\ell}$ and $k_{F,x\geqslant 0} = k_{Fr}$. In this system backscattering can be rewritten as

$$\begin{aligned}\hat{H}' &\approx \lambda e^{-i\sqrt{4\pi}\phi(x=0)} + \text{H.c.},\\ \lambda &= -i\sum_x \frac{1}{2\pi a} e^{-2ik_{F,x}x}\left[\frac{e^{-i\kappa_x^-}u_x}{\sin[\kappa_x^-]} - Va\right].\end{aligned} \tag{3.12}$$

With the help of Appendix E, and noting that for an abrupt jump $\kappa_x^- = k_{F,x}a$, we have to lowest order in the interaction

$$\begin{aligned}\lambda \approx \frac{1}{2\pi}&\left[\frac{t_\ell}{\sin[k_{F\ell}a]} + \frac{U_\ell}{\pi} - \frac{t_r}{\sin[k_{Fr}a]} - \frac{U_r}{\pi}\right]\\ &- \frac{V}{4\pi}[\cot[k_{F\ell}a] - \cot[k_{Fr}a]],\end{aligned} \tag{3.13}$$

which generalizes the noninteracting result, Eq. (2.12). As λ is real we find that there is no $\sin[\sqrt{4\pi}\phi(0)]$ operator present at the boundary and the total backscattering is

$$\hat{H}' = 2\lambda\cos[\sqrt{4\pi}\phi(0)]\,. \tag{3.14}$$

The perhaps surprising absence of the $\sin[\sqrt{4\pi}\phi(0)]$ operator is connected to the local properties of the Hamiltonian in the vicinity of the boundary, see Appendix B. As such there remains only one condition to fulfill for the conducting fixed point: $\lambda = 0$ with λ real.

For $V = 0$ when there is particle-hole symmetry present, corresponding to the mapping $\phi \to -\phi$ and $\tilde{\phi} \to -\tilde{\phi}$, it is transparent that $\sin[\sqrt{4\pi}\phi(0)]$ is forbidden. For $V \neq 0$ we find that λ remains real for the specific junction considered—analytically to first order in the interaction U, see Eq. (3.13), and numerically for all interactions strengths, see below. We do not have a simple argument why this is the case and Appendix B shows that this is in fact not a generic feature of an abrupt junction.

B. Local density and compressibility

For the system with an abrupt jump in hopping and interaction strength it is possible to calculate a variety of properties perturbatively in the boundary operators using the exact Green's function for the Hamiltonian (3.8), see Eq. (D2) in the Appendix. In addition to the dc conductance one can also consider local properties such as the local density and compressibility of the wire. For abrupt changes in parameters the local density is known to show characteristic oscillations, the Friedel oscillations [33], which give information about the interacting correlation functions [34–36] and the strength of the backscattering [27,37].

The bosonized density operator for the fermions becomes

$$\begin{aligned}n(x) = n_0(x) &- \frac{1}{\sqrt{\pi}}\partial_x\phi(x)\\ &+ \frac{\text{const.}}{\pi}\sin[2k_{F,x}^* x + \sqrt{4\pi}\phi_x]\,.\end{aligned} \tag{3.15}$$

As before we keep the local potential energy constant $V_x = V$. The oscillating contribution to the density, i.e., the Friedel oscillations, which are given by

$$\rho_{\text{alt}}(x) \equiv \left\langle \frac{\text{const.}}{\pi}\sin[2k_{F,x}^* x + \sqrt{4\pi}\phi(x)]\right\rangle, \tag{3.16}$$

will be calculated to first order in λ. $k_{F,x}^*$ is the renormalized Fermi momentum at finite temperature which can be found from the bulk density: $\rho_x \equiv \langle n_{0,x}\rangle = k_{F,x}^*/\pi$.

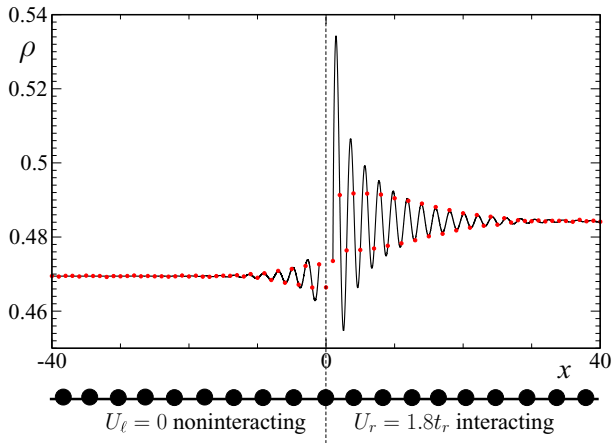

FIG. 1. (Color online) The full density including Friedel oscillations near the boundary, numerical results (filled circles) are fitted to the analytical result of Eq. (3.19) (lines) with $t_l = 1.308t_r$, $U_\ell = 0$, and $U_r = 1.8t_r$. The local potential energy is $V = -0.25t_r$ and $t_r\beta = 10$. Underneath a schematic of the system under consideration is shown.

For this we require the following integral

$$\begin{aligned}\tau(x) &\equiv 2\int_0^\beta d\tau\,\langle\cos[\sqrt{4\pi}\phi(x,0)]\cos[\sqrt{4\pi}\phi(0,\tau)]\rangle \\ &= \int_0^\beta d\tau e^{2\pi[G(x,0;\tau)-G(0,0;0)]} \\ &= \frac{1}{T}\left(\frac{4\pi Ta}{u_x}\right)^{\bar{g}}\left(\frac{u_x}{2\pi aT}\sinh\left[\frac{2\pi Tx}{u_x}\right]\right)^{-g_x} P_{-\bar{g}}(z),\end{aligned} \tag{3.17}$$

which has been calculated using the Green's function in Appendix D. We introduced

$$z \equiv \coth\left[\frac{2\pi Tx}{u_x}\right], \tag{3.18}$$

and $P_l(z)$ is the Legendre function. This gives

$$\begin{aligned}\rho_{\rm alt}(x) &= -\frac{\text{const.}}{\pi}\int_0^\beta d\tau\,\langle\sin[2k^*_{F,x}x + \sqrt{4\pi}\phi(x)]\hat{H}'\rangle \\ &= -\lambda\frac{\text{const.}}{\pi^2 a}\tau(x)\sin[2k^*_{F,x}x].\end{aligned} \tag{3.19}$$

To test the calculations we have developed a quantum Monte Carlo (QMC) code using a stochastic series expansion (SSE) with directed loops [38,39]. In Figs. 1 and 2 we show a comparison of this analytical result with the outcome of QMC simulations on spinless fermions. Even for a very large jump in parameters the fit remains very good. Note that what is seen in the local density and compressibility profiles, see below, is an interplay between the shape of $\tau(x)$ and the incommensurate oscillations from $\sin[2k^*_{F,x}x]$. For the fitting procedure between the analytical and numerical results there are two parameters. The first is the amplitude of the effect due to the unknown constant in Eq. (3.16) and the cutoffs in the field theory. The second is a small offset in position, $\rho_{\rm alt}(x-\bar{a})$, due to an effective width of the scattering center,

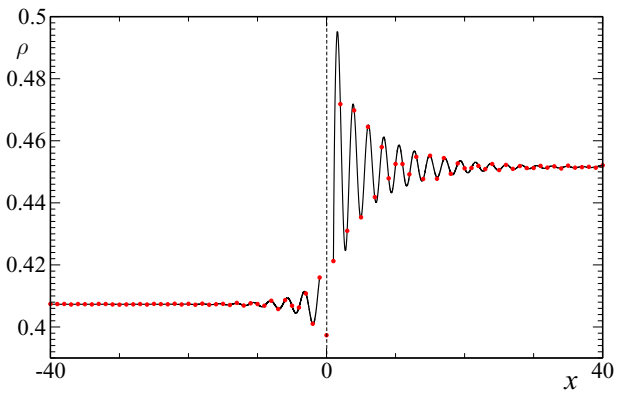

FIG. 2. (Color online) The full density including Friedel oscillations near the boundary, numerical results (filled circles) are fitted to the analytical result of Eq. (3.19) (lines) with $t_l = 1.31t_r$, $U_\ell = 0$, and $U_r = 1.8t_r$. The local potential energy is $V = -0.75t_r$ and $t_r\beta = 10$.

with $\bar{a}$ being of the order of the lattice spacing a. The Luttinger parameters $g_{\ell,r}$ can be found from the Bethe ansatz [40–43].

The local compressibility is defined as

$$\chi_x = -\left.\frac{\partial\langle\hat{n}_x\rangle}{\partial\delta V}\right|_{\delta V=0}, \tag{3.20}$$

analogous to the local susceptibility in a spin chain [35]. For the alternating contribution this yields

$$\chi_{\rm alt} \propto \lambda x\tau(x)\cos[2k^*_{F,x}x]. \tag{3.21}$$

Unlike the Friedel oscillations in the density this observable remains nonzero even for half-filling and is therefore in that particular case a more useful quantity to study.

C. Conducting fixed points

In Sec. III A we have predicted that for the abrupt junction considered only one parameter needs to be tuned to find a conducting fixed point. The low-order expansion for λ given by Eq. (3.13) is not sufficient, however, to find the location of the fixed points for the large interaction strengths we want to consider in general. Only in the limit $U_x \to 0$, where we know the exact result, can we be confident of its predictions. An exception is the half-filled case where we have previously argued [27] that the scattering amplitude λ vanishes for all interaction strengths if $u_\ell = u_r$, with the velocities at half-filling known in closed form as a function of the interaction strength from Bethe ansatz [40,41].

Instead, at generic fillings, we can find the locations of the solutions $t^*(V)$ which solve $\lambda(t_\ell = t^*, V) = 0$, keeping U_x and t_r fixed, by analyzing the local density or compressibility of the system by QMC simulations described in the preceding subsection. We find that, away from half-filling, these *do not* correspond to $u_\ell = u_r$. For $\lambda = 0$ the density is determined entirely by the Hamiltonian Eq. (3.8), plus irrelevant perturbations. For $\lambda \neq 0$, on the other hand, the relevant backscattering term contributes. By plotting the density for different t_ℓ in Fig. 3 we can find the places where the leading corrections vanish and λ changes sign [27], which typically can be observed in the range $5a \lesssim x \lesssim 10a$. Since we can always identify a value of hopping where the leading contribution

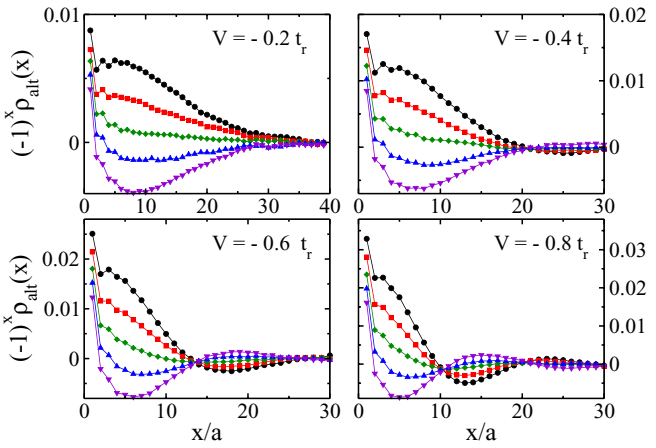

FIG. 3. (Color online) Plotted are the Friedel oscillations for different local potential energies V calculated by QMC simulations, see main text for details, on the right-hand side of the junction ($x > 0$). We only show the longer wavelength amplitude of the rapid oscillations. In each panel from top to bottom: $t_\ell = 1.3t_r$ for (black) circles, $t_\ell = 1.4t_r$ for (red) squares, $t_\ell = 1.5t_r$ for (green) diamonds, $t_\ell = 1.6t_r$ for (blue) up-triangles, and $t_\ell = 1.7t_r$ for (purple) down-triangles. We have used everywhere $U_\ell = 0$, $U_r = 1.8t_r$ and inverse temperature $t_r\beta = 10$.

vanishes, there must be a line of conducting fixed points in parameter space. In turn the existence of a full line of fixed points demonstrates that there is only one condition for the conducting fixed point, $\lambda = 0$ with real λ. We want to stress though that even at such a point in parameter space there are still irrelevant backscattering processes present which only vanish in the zero temperature limit $\beta \to \infty$.

IV. CONFORMALLY INVARIANT BOUNDARY THEORY

In the preceding sections it has been demonstrated that it is possible to find an unstable conducting fixed point in two wires connected at a junction by appropriately tuning the bulk parameters of the wires. The existence of this fixed point immediately invites the question of the nature of the effective low energy theory. Obviously translational invariance is lost and it is also not possible to use mirror charges as would be the case for an open boundary condition. Therefore it is highly nontrivial to postulate a description in terms of a conformally invariant theory in this case. Nonetheless, as we will show in this section it is possible to characterize this fixed point in terms of mode expansions and *two* effective boundary Luttinger liquid parameters. Particular attention is paid to the case of half-filling where we can pinpoint the fixed point precisely. This allows convenient numerical checks of the results.

A. Mode expansion and finite size spectrum

In the absence of backscattering at a junction we have the bosonic Hamiltonian [17,27,30]

$$\hat{H} = \int dx \frac{1}{2}\left(\frac{1}{g_x}(\partial_x\phi)^2 + g_x(\partial_x\tilde{\phi})^2\right). \tag{4.1}$$

Compared to Eq. (3.8) the position x was rescaled on the two sides of the junction such that $u_\ell, u_r \to 1$. The fields obey the canonical commutation relation: $[\phi(x), \partial_y\tilde{\phi}(y)] = i\delta(x-y)$. Therefore we have the relation

$$\partial_t\phi(x) = i[H,\phi(x)] = g_x\partial_x\tilde{\phi}(x)\,. \tag{4.2}$$

The corresponding Green's function can be determined from Eq. (4.1), see Eq. (D2). Here we explore other properties of this boundary condition. We are interested in the solutions of the classical equation of motion,

$$\left[\partial_t^2 - g_x\partial_x\left(\frac{1}{g_x}\partial_x\right)\right]\phi(x,t) = 0 \tag{4.3}$$

on a ring with circumference $2L$ where

$$g_x = \begin{cases} g_\ell & \text{if } -L < x < 0, \\ g_r & \text{if } 0 < x < L\,. \end{cases} \tag{4.4}$$

At the boundaries $\phi(x)$ and $\partial_x\phi(x)/g_x$ have to be continuous leading to the boundary conditions

$$\begin{gathered} \phi(0^-) = \phi(0^+), \quad \phi(-L) = \phi(L), \\ \frac{\partial_x\phi(0^-)}{g_\ell} = \frac{\partial_x\phi(0^+)}{g_r}, \quad \frac{\partial_x\phi(-L)}{g_\ell} = \frac{\partial_x\phi(L)}{g_r}. \end{gathered} \tag{4.5}$$

The classical equation of motion (4.3) has oscillatory solutions as well as solutions linear in x, see Appendix F for details. We may expand the field $\phi(x)$ in these solutions, while respecting the canonical commutation relation

$$[\phi(x), \partial_t\phi(y)] = ig_x\delta(x-y)\,. \tag{4.6}$$

This leads to

$$\phi(x,t) = \phi_0 + \frac{\bar{g}\Pi t}{2L} + \frac{Qxg_x}{2\bar{\gamma}L} + \sum_{l=1}^{\infty}\left[\frac{e^{-i\pi lt/L}}{\sqrt{2\pi l}}\left[\sqrt{\bar{g}}\cos(\pi lx/L)a_{e,l} + \frac{g_x}{\sqrt{\bar{\gamma}}}i\sin(\pi lx/L)a_{o,l}\right] + \text{H.c.}\right], \tag{4.7}$$

$$\tilde{\phi}(x,t) = \tilde{\phi}_0 + \frac{1}{\bar{\gamma}}\frac{Qt}{2L} + \frac{\bar{g}\Pi x}{2g_xL} - \sum_{l=1}^{\infty}\left[\frac{e^{-i\pi lt/L}}{\sqrt{2\pi l}}\left[\frac{\sqrt{\bar{g}}}{g_x}i\sin(\pi lx/L)a_{e,l} + \frac{1}{\sqrt{\bar{\gamma}}}\cos(\pi lx/L)a_{o,l}\right] + \text{H.c.}\right].$$

As before we have the boundary Luttinger parameter

$$\frac{1}{\bar{g}} = \frac{1}{2}\left[\frac{1}{g_\ell} + \frac{1}{g_r}\right], \tag{4.8}$$

which describes the conductance [16,27,30]. Interestingly, we find in addition a second boundary Luttinger parameter

$$\bar{\gamma} = \tfrac{1}{2}\left[g_\ell + g_r\right], \tag{4.9}$$

which is important for other correlation functions as we will see below. Π is the field conjugate to ϕ_0 with $[\phi_0,\Pi]=i$. As this field is periodic, $\phi_0 \to \phi_0+\sqrt{\pi}$, it is clear that the eigenvalues of the conjugate field Π must be $2\sqrt{\pi}m$, where m is an integer. Q is the field conjugate to $\tilde{\phi}_0$ and $\tilde{\phi}_0 \to \tilde{\phi}_0+\sqrt{4\pi}$ so that the eigenvalues of the conjugate field Q are $\sqrt{\pi}n$ for integer n.

The classical equation of motion (4.3) has to follow from a classical least action principle from which the classical Hamiltonian

$$H=\int_0^{2L}\frac{dx}{2g_x}[(\partial_t\phi)^2+(\partial_x\phi)^2] \tag{4.10}$$

is determined. Substituting the mode expansion into the Hamiltonian, we may read off the finite size spectrum

$$E=\frac{\pi}{L}\left[-\frac{1}{12}+\frac{n^2}{4\bar{\gamma}}+m^2\bar{g}+\sum_{l=1}^{\infty}l(m_{e,l}+m_{o,l})\right]. \tag{4.11}$$

Here n and m are arbitrary integers while $m_{e/o,l}$ are nonnegative integers corresponding to the eigenvalues of $a^\dagger_{e/o,l}a_{e/o,l}$. We have included the universal term in the ground state energy $-c\pi/(12L)$ with $c=1$ for a periodic system of length $2L$.

B. Scaling properties of the conducting fixed point

As usual, since we have imposed the same boundary condition at both ends, we may read off the scaling dimensions of all single-valued boundary operators in the bosonized theory from the finite size spectrum. The scaling dimensions are

$$\zeta_{m,n}=\frac{n^2}{4\bar{\gamma}}+m^2\bar{g}+\sum_{l=1}^{\infty}l(m_{e,l}+m_{o,l}). \tag{4.12}$$

Each dimension corresponds to a different boundary operator. $m^2\bar{g}$ corresponds to $\exp[im\sqrt{4\pi}\phi(0)]$ with the $m=\pm1$ operators being the leading relevant operators at the unstable fixed point. $\bar{\gamma}/4$ is the dimension of the operators $\exp[\pm i\sqrt{\pi}\tilde{\phi}(0)]$, which effectively correspond to spin operators $S^{\pm}(x=0)$, see below.

To analyze the scaling properties of the system, and compare the results to numerical calculations, it is convenient to introduce correlation functions for a spin system equivalent to our fermionic system. The mapping between spin operators and fermionic operators is given by the Jordan-Wigner transformation

$$S^+_j=\psi^\dagger_j e^{i\pi\sum_{l<j}\psi^\dagger_l\psi_l}. \tag{4.13}$$

The leading S^+S^- correlation function at the boundary $x=0$ is, in bosonized form,

$$\langle S^+(0,t)S^-(0,0)\rangle \sim \langle e^{-i\sqrt{\pi}\tilde{\phi}(0,t)}e^{-i\sqrt{\pi}\tilde{\phi}(0,0)}\rangle. \tag{4.14}$$

Using Eq. (4.7) this results in

$$\langle S^+(0,t)S^-(0,0)\rangle \sim \left|\frac{\sin[\pi t/2L]}{\sin[\pi a/2L]}\right|^{-\frac{1}{2\bar{\gamma}}}, \tag{4.15}$$

with the boundary exponent $\bar{\gamma}$. For the S^z operator we have after bosonization

$$S^z_j=\psi^\dagger_j\psi_j-\frac{1}{2}=-\frac{a}{\sqrt{\pi}}\partial_x\phi+(-1)^j\text{const}\times\sin[\sqrt{4\pi}\phi]. \tag{4.16}$$

The leading S^z spin density waves are described by the autocorrelation function at the boundary

$$\langle S^z(0,t)S^z(0,0)\rangle \sim \sum_{\alpha=\pm}\langle e^{i\alpha\sqrt{4\pi}[\phi(0,t)-\phi(0,0)]}\rangle. \tag{4.17}$$

From this one finds

$$\langle S^z(0,t)S^z(0,0)\rangle \sim \left|\frac{\sin[\pi t/2L]}{\sin[\pi a/2L]}\right|^{-2\bar{g}}, \tag{4.18}$$

with the boundary exponent $\bar{g}$. Thus the boundary theory is described by *two different* boundary Luttinger parameters, $\bar{g}$ and $\bar{\gamma}$.

In the QMC simulations we consider finite temperatures in the limit of large system sizes $L\gg u\beta$ and calculate the imaginary time correlation functions. In this case the results are most easily accessible by considering the Green's function Eq. (D2), and the equivalent correlation function for the adjoint field $\tilde{\phi}(x,\tau)$. Then we find

$$C_\pm(\tau)\equiv\langle S^+(0,\tau)S^-(0,0)\rangle \sim \left|\frac{\sin[\pi\tau/\beta]}{\pi a/\beta}\right|^{-\frac{1}{2\bar{\gamma}}}, \tag{4.19}$$

and

$$C_z(\tau)\equiv\langle S^z(0,\tau)S^z(0,0)\rangle \sim \left|\frac{\sin[\pi\tau/\beta]}{\pi a/\beta}\right|^{-2\bar{g}}. \tag{4.20}$$

We compare the predicted scaling of these correlation functions to the results of QMC simulations. The predicted exponents are well verified, see Fig. 4. Not only can one clearly distinguish the two boundary exponents, but we have also checked that the bulk exponents do not fit the scaling. Note

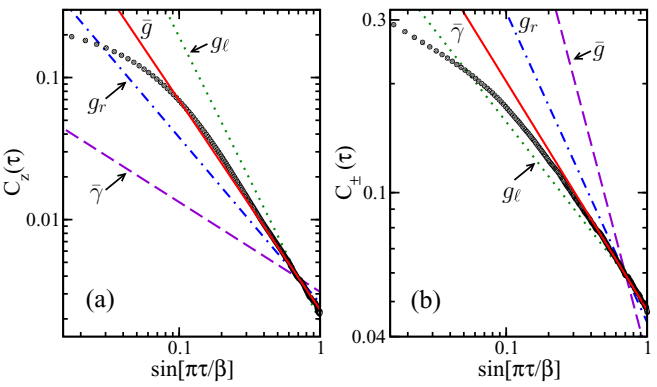

FIG. 4. (Color online) The scaling of the local spin correlation functions $C_z(\tau)$ and $C_\pm(\tau)$ at the fixed point: $t_\ell=1.518t_r$, $U_\ell=0$, and $U_r=1.8t_r$. The magnetic field is zero (i.e., $V=0$ for the corresponding fermion system) and the temperature is $t_r\beta=25$. (a) Numerical data, black circles, are compared to the predicted scaling $f(\tau)^\nu$ with $f(\tau)\equiv|\sin(\pi\tau/\beta)|^{-2}$ and $\nu=\bar{g}$ (red curve). As a comparison we also plot $f(\tau)^\nu$ with $\nu=g_\ell, g_r, \bar{\gamma}$, see Eq. (4.20). (b) Numerical data, black circles, are compared to the predicted scaling $f(\tau)^{1/4\nu}$ with $\nu=\bar{\gamma}$ (red curve). As a comparison we also plot $f(\tau)^{1/4\nu}$ with $\nu=g_\ell, g_r, \bar{g}$, see Eq. (4.19).

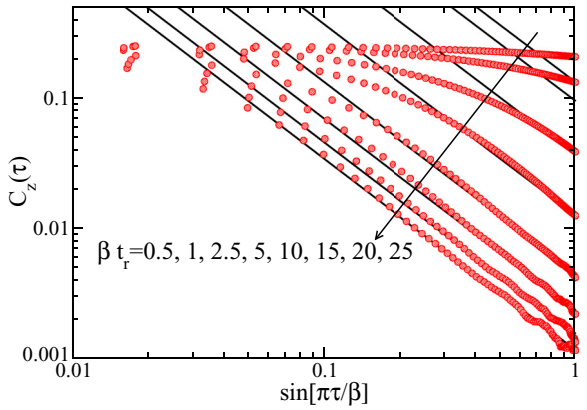

FIG. 5. (Color online) The scaling of the local spin correlation function $C_z(\tau)$ at the conducting fixed point with $t_\ell = 1.518t_r$, $U_\ell = 0$, and $U_r = 1.8t_r$. The magnetic field is zero (i.e., $V = 0$ for the corresponding fermion system). Numerical data for different inverse temperatures (as indicated on the plot) are compared to the predicted scaling (lines). As temperature is lowered the field theory becomes more accurate.

that the analytical formula are only valid in the asymptotic limit $\tau \gg \beta$. The values of $g_{\ell,r}$, and hence of $\bar{\gamma}$ and $\bar{g}$, can be found exactly from the results of the Bethe ansatz [40–43].

Figure 5 shows the temperature scaling of $C_z(\tau)$ at the conducting fixed point $t_\ell = 1.518t_r$, and Fig. 6 the scaling away from it. At the conducting fixed point the field theory, as expected, does not describe the data at high temperatures, such as $t_r\beta = 0.5$ or $t_r\beta = 2.5$. As temperature is lowered the field theory becomes a better and better fit, showing good scaling already by $t_r\beta = 5$. As we move away from the conducting fixed point the corrections to scaling are expected to grow while lowering the temperature but are only $O(\lambda^2)$. This makes it impossible to see the approach to the insulating fixed point in $C_z(\tau)$. The Friedel oscillations of the density and compressibility considered in Sec. III B are, in principle, better to see the crossover to the insulating fixed point. However, the expected cross-over temperature is of order $T \approx 10^{-4}t_r$

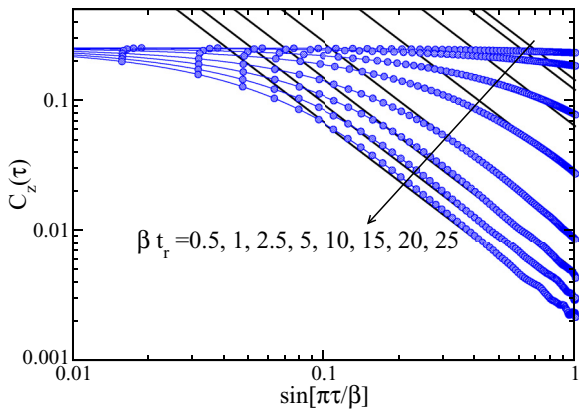

FIG. 6. (Color online) The scaling of the local spin correlation function $C_z(\tau)$ away from the conducting fixed point with $t_\ell = t_r$, $U_\ell = 0$, and $U_r = 1.8t_r$. The magnetic field is zero (i.e., $V = 0$ for the corresponding fermion system). From top to bottom we plot different values of the inverse temperature $t_r\beta = \{0.5, 2.5, 5, 10, 15, 20, 25\}$.

(Ref. [27]), which is unfortunately well beyond the reach of the numerical QMC simulations.

C. Local density of states

One possible experimental test on boundary exponents is the measurement of the local density of states with local spectroscopic tools, such as scanning tunneling spectroscopy [44]. Theoretically a characteristic depletion with the boundary exponent has been predicted [9,45–49], which may be corrected by irrelevant operators [50]. It is therefore interesting to calculate the characteristic signatures of the local density of states for this unusual fixed point.

The local density of states is defined as

$$\nu(x,\omega) = \frac{1}{\pi}\int dt e^{i\omega t}\mathrm{Re}\langle\psi(x,t)\psi^\dagger(x,0)\rangle = \frac{1}{2\pi^2 a}\int dt e^{i\omega t}\sum_{\alpha=\pm} e^{-2\pi\langle(\phi_\alpha(x,t)-\phi_\alpha(x,0)bm)^2\rangle}. \tag{4.21}$$

Using the correlation functions calculated from the mode expansion, see Appendix F, and, neglecting the cutoff for the moment, this results in

$$\nu(x,\omega) \sim \frac{1}{2\pi^2 a}\int dt e^{i\omega t}|4\sin^2[\pi t/2L]|^{-\delta_x} \times |4\sin[\pi(t-2x)/2L]\sin[\pi(t+2x)/2L]|^{-\kappa_x} \times \sum_{\alpha=\pm}\left|\frac{\sin[\pi(t-2x)/2L]}{\sin[\pi(t+2x)/2L]}\right|^{\alpha/2}. \tag{4.22}$$

The exponents are given by

$$\kappa_x = \frac{1}{8}\left[\bar{g}+\frac{1}{\bar{\gamma}}-\frac{\bar{g}}{g_x^2}-\frac{g_x^2}{\bar{\gamma}}\right] = \frac{1}{4}\frac{g_x-g_{-x}}{g_\ell+g_r}\left(\frac{1}{g_x}-g_x\right), \quad \delta_x = \frac{1}{8}\left[\bar{g}+\frac{1}{\bar{\gamma}}+\frac{\bar{g}}{g_x^2}+\frac{g_x^2}{\bar{\gamma}}\right] = \frac{1}{4}\left(\frac{1}{g_x}+g_x\right). \tag{4.23}$$

In the bulk regions near $x \approx L/2$ we recover $\nu(0,\omega) \sim |\omega|^{\xi_x}$ with the usual exponents $\xi_x = 2\delta_x - 1$.

The local density of states at the boundary $x = 0$ therefore becomes, reinstating a cutoff of the order of the lattice spacing a,

$$\nu(0,\omega) \sim \frac{1}{\pi^2 a}\int dt e^{i\omega t}\left|\frac{\sin[\pi t/2L]}{\pi a/2L}\right|^{-2\zeta} \tag{4.24}$$

giving $\nu(0,\omega) \sim |\omega|^{2\zeta-1}$ with scaling dimension

$$\zeta \equiv \frac{1}{4}\left[\bar{g}+\frac{1}{\bar{\gamma}}\right] = \frac{1+g_\ell g_r}{2(g_\ell+g_r)}. \tag{4.25}$$

Note that this is *not* one of the dimensions of single-valued operators, $\exp[i\sqrt{\pi}(n\tilde{\phi}+2m\phi)]$ for integer n, m listed in Eq. (4.12). Rather $\psi_\pm \propto \exp[i\sqrt{\pi}(\pm\tilde{\phi}+\phi)]$, corresponding to $n = \pm 1$, $m = 1/2$. The non-single-valued nature of these operators is a result of their being fermonic. ζ is the same as the bulk scaling dimension in a homogeneous spinless Luttinger liquid with $g \to \bar{g}$ and $g^{-1} \to \bar{\gamma}^{-1}$. Surprisingly, the density of states at the junction scales as in the free fermion case if either side of the junction is noninteracting: $g_\ell = 1$

or $g_r = 1$. This can be understood from the density of states, Eq. (4.22), if we have $g_\ell = 1$ then the exponent $\kappa_{x<0} = 0$. Both in the vicinity of the boundary and in the bulk the last line in Eq. (4.22) does not affect the scaling properties of the density of states. Hence the scaling of $\nu(x < 0,\omega)$ on the noninteracting side is no longer position dependent and shows the bulk scaling right up to the boundary itself. This is not true on the interacting side ($x > 0$) where the scaling modulates from the noninteracting result at the boundary $x = 0$, to the bulk interacting value far inside the wire. In contrast to the density or compressibility of Sec. III B there is no proximity effect near the boundary in the noninteracting wire.

D. Fixed points and the *g* theorem

From the finite size spectrum, Eq. (4.11), we may also read off the partition function in the scaling limit:

$$Z(\beta/L) = \eta^{-2}(e^{-\pi\beta/L})\theta_3(e^{-\pi\beta/[2\bar{\gamma}L]})\theta_3(e^{-\pi\beta 2\bar{g}/L})\,. \quad (4.26)$$

Here we have introduced the Dedekind eta and Jacobi theta functions,

$$\eta(q) \equiv q^{1/24}\prod_{n=1}^{\infty}(1-q^n) \quad \text{and}$$
$$\theta_3(q) \equiv \sum_{n=-\infty}^{\infty} q^{n^2/2}\,. \quad (4.27)$$

In the thermodynamic limit, $\beta/L \to 0$, this becomes

$$Z \to \sqrt{\bar{\gamma}/\bar{g}}\,e^{\pi L/(3\beta)}\,. \quad (4.28)$$

Apart from the usual bulk free energy, $F = -\pi L/(3\beta^2)$, there is also a "ground state degeneracy" g_d associated with the two interfaces in the system. The factor for each interface is

$$g_d^c = \left(\frac{\bar{\gamma}}{\bar{g}}\right)^{\frac{1}{4}} = \frac{(g_\ell + g_r)^{1/2}}{(4g_\ell g_r)^{1/4}}\,. \quad (4.29)$$

This may be compared to the ground state degeneracy for the insulating fixed point where the junction consists of the perfectly reflecting ends of two quantum wires with Luttinger parameters g_ℓ and g_r. This fixed point has [11]

$$g_d^i = (g_\ell g_r)^{1/4}\,, \quad (4.30)$$

According to the "*g* theorem," boundary RG flows between fixed points can only occur when g_d is reduced during the flow [51]. Therefore, it is interesting to consider the ratio

$$g_d^c/g_d^i = \frac{1}{\sqrt{\bar{g}}}\,. \quad (4.31)$$

The *g* theorem states that flow from the conducting to insulating fixed point is only possible when $\bar{g} < 1$. This is consistent with the analysis here since $\bar{g}$ is the dimension of the operator $\cos[\sqrt{4\pi}\phi(0)]$ which drives the flow. The flow only takes place when the operator is relevant, corresponding to $\bar{g} < 1$. For sufficiently large g_d^i the renormalization flow can occur from insulating to conducting fixed points. As shown in Ref. [11], the fermion operator, or equivalently spin raising operator, at the end of the open chain, has scaling dimension $1/(2g_\ell)$ or $1/(2g_r)$ as appropriate. We might expect the flow from insulating to conducting when the tunneling between the two open chains is relevant which occurs when

$$\frac{1}{2g_\ell} + \frac{1}{2g_r} = \frac{1}{\bar{g}} < 1 \quad (4.32)$$

and hence $\bar{g} > 1$. In this case $g_d^c < g_d^i$ so this flow is also consistent with the *g* theorem.

It is also interesting to consider the flow starting from the insulating fixed point, but with a weakly connected resonant site in between the two wires: the resonant fixed point. Then for a range of Luttinger parameters an RG flow from the resonant to the conducting fixed point is expected. A necessary condition for the flow from resonant to conducting fixed points is that the tunneling operators from each chain to the resonant site are relevant, $g_{\ell,r} > 1/2$. The ground state degeneracy of the resonant fixed point is bigger by a factor of 2 than that of the insulating fixed point due to the two-fold degeneracy of the resonant site and

$$g_d^r = 2(g_\ell g_r)^{1/4}\,. \quad (4.33)$$

Thus the ratio of ground state degeneracies of the resonant to conducting fixed points is

$$g_d^r/g_d^c = 2\sqrt{\bar{g}}\,. \quad (4.34)$$

We can see that $g_d^r/g_d^c \geqslant \sqrt{2}$ whenever $g_\ell, g_r > 1/2$ so the *g* theorem is also obeyed by this RG flow. Even when λ is tuned to zero, corresponding to resonance, the next most relevant operators, $\exp[\pm 2i\sqrt{4\pi}\phi(0)]$ will still be present. This can drive the flow from the conducting to the resonant fixed points when it becomes relevant, i.e., for $4\bar{g} < 1$. Since $g_d^c/g_d^r = 1/(2\sqrt{\bar{g}})$ we see that this flow is consistent with the *g* theorem as it only occurs when $\bar{g} < 1/4$. Therefore all expected RG flows are consistent with the *g* theorem.

As first observed by Kane and Fisher [9] in the case $g_\ell = g_r$, there is a range of Luttinger parameters where both conducting and resonant fixed points are stable. In this case they are separated by an intermediate unstable fixed point.

V. CONCLUSION

In conclusion, we have described a novel conducting fixed point in inhomogeneous quantum wires. This fixed point is reached by tuning to zero the amplitude of the leading backscattering operator at the junction between two homogeneous parts of the wire. We have, in particular, studied a lattice model of spinless fermions with nearest-neighbor hopping and interaction in the critical regime. For the case of an abrupt junction we have derived the backscattering amplitude for all fillings in lowest order in the interaction. For the half-filled case it is even possible to give a condition for the vanishing of the backscattering amplitude valid for all interaction strengths. The prediction of a conducting fixed point were numerically confirmed by QMC calculations of the Friedel oscillations in the local density and compressibility close to the boundary which vanish in leading order at the fixed point.

One of our main results is the derivation of the boundary conformal field for this novel unstable conducting fixed point. The conformally invariant theory for this case is highly unusual

because the two parts of the wire are governed by different bulk Luttinger parameters g_ℓ and g_r. As a consequence, we find that the scaling dimensions of boundary operators are also governed by two different Luttinger parameters given by $\bar{\gamma} = (g_\ell + g_r)/2$ and $\bar{g} = 2g_\ell g_r/(g_\ell + g_r)$. We showed, both analytically and numerically that $\bar{\gamma}$ is controlling the transverse spin autocorrelation function while $\bar{g}$ controls the longitudinal one in the corresponding spin model. Experimentally, a test of the boundary exponents could possibly be obtained by scanning tunneling microscopy which would allow one to measure the local density of states which shows energy scaling with an exponent being determined by $\bar{\gamma}$ and $\bar{g}$.

ACKNOWLEDGMENTS

J.S., S.E., and N.S. acknowledge support by the Collaborative Research Center SFB/TR49 and the graduate school of excellence MAINZ. The research of I.A. was supported by NSERC and CIfAR. We are grateful for computation time at AHRP.

APPENDIX A: LANDAUER FORMULA FOR TRANSMISSION

The significance of the measure of transmission $R = 0$ can be verified by considering the Landauer formula [52]. Thus we imagine attaching the wire to reservoirs on the left and right sides with different chemical potentials μ_L and μ_R. We consider particles emitted from the left reservoir with a thermal distribution with chemical potential $\mu_L = -eV_L$ and from the right reservoir with a thermal distribution and chemical potential $\mu_R = -eV_R$. At zero temperature the Fermi wave vectors on the left and right sides, $k_{F\ell}$ and k_{Fr}, are given by

$$-2t\cos k_{F\ell,r} - \mu_{\ell,r} = \mu_{L,R}\,. \tag{A1}$$

Suppose that the bottom of the band on the left has higher energy than the bottom of the band on the right. Then the total current, at zero temperature, is

$$I = -e\int_0^{k_{F\ell}} \frac{\mathrm{d}k}{2\pi} u_\ell(k)[1-|R(k)|^2] + e\int_{-k_{Fr}}^{-k_{2\max}} \frac{\mathrm{d}k}{2\pi} u_\ell(k)|T(k)|^2\,. \tag{A2}$$

The first term is the current emitted by the left reservoir and partially reflected at the interface. The second term is the current emitted by the right reservoir and partially transmitted. The maximum wave vector for the second integral, $k_{2\max} > 0$, is given by $\epsilon_2(-k_{2\max}) = \epsilon_1(0)$ since lower energy incoming particles from the right have zero transmission probability.

It is convenient to change integration variables to ϵ_1 in the first integral and ϵ_2 in the second, giving:

$$I = -e\int_{\epsilon_1(0)}^{\mu_L} \frac{d\epsilon_1}{2\pi}[1-|R(\epsilon_1)|^2] + e\int_{\epsilon_1(0)}^{\mu_R} \frac{d\epsilon_2}{2\pi}\frac{u_\ell(\epsilon_2)}{u_r(\epsilon_2)}|T(\epsilon_2)|^2. \tag{A3}$$

Since $|T|^2 u_\ell/u_r = 1 - |R|^2$ this can be written as

$$I = -e\int_{\mu_R}^{\mu_L} \frac{d\epsilon}{2\pi}[1-|R(\epsilon)|^2]\,. \tag{A4}$$

Now taking the limit $\mu_L \to \mu_R \equiv \epsilon_F$, we find

$$I \to \frac{e^2}{2\pi}[1-|R(\epsilon_F)|^2](V_L - V_R)\,. \tag{A5}$$

Hence the linear conductance is

$$G = \frac{dI}{dV} = \frac{e^2}{2\pi}[1-|R(\epsilon_F)|^2]\,. \tag{A6}$$

This is another way of seeing that $[1-|R|^2]$ is the suitable measure of the transmission of the interface.

APPENDIX B: NONINTERACTING CALCULATIONS

In the main text in Sec. II we have considered the simplest possible junction, a jump between two homogeneous regions, in the noninteracting case. Here we want to present calculations for more general junctions to study the influence on the backscattering term.

1. Abrupt junction with additional local variation

The calculation of Sec. II can be extended straightforwardly to a more general model where the hopping amplitude varies near the origin. Suppose, for example, that the hopping amplitude from site -1 to 0 is $t_{-1} = t'_\ell$ and from 0 to 1 is $t_0 = t'_r$ with the rest as given by Eq. (2.7). For simplicity we concentrate again on half-filling, $V_j = 0$. Then we may write the wave function for an incoming wave from the left as in Eq. (2.3) with $j_\ell = -1$ and $j_r = 1$. ψ_0 is now a free parameter. Solving for the reflection amplitude as previously gives

$$|R|^2 = \frac{\left[\frac{t'^2_\ell}{t^2_\ell}u_\ell - \frac{t'^2_r}{t^2_r}u_r\right]^2 + a^2\epsilon^2\left[2 - \frac{t'^2_\ell}{t^2_\ell} - \frac{t'^2_r}{t^2_r}\right]^2}{\left[\frac{t'^2_\ell}{t^2_\ell}u_\ell + \frac{t'^2_r}{t^2_r}u_r\right]^2 + a^2\epsilon^2\left[2 - \frac{t'^2_\ell}{t^2_\ell} - \frac{t'^2_r}{t^2_r}\right]^2}\,. \tag{B1}$$

Solving for $R = 0$ one finds

$$(t'_\ell/t_\ell, t'_r/t_r) = \sqrt{2}(\cos\theta, \sin\theta) \tag{B2}$$

with $\tan^2\theta = u_\ell/u_r$. Thus maximal conductance can be achieved for any choice of energy ϵ, and thus any value of u_ℓ/u_r that can occur as ϵ is varied.

We see that the simple condition $u_\ell = u_r$ for perfect conductance is a special result, which only holds for the "abrupt junction" considered in the main text. In general, the condition $u_\ell = u_r$ can be regarded as removing the intrinsic scattering from a sharp jump between bulk values of the hopping. Additional variation on top of this will naturally result in scattering and an additional fine-tuning is required to reach the conducting fixed point.

Note that the fact that two parameters t'_ℓ and t'_r need to be adjusted to achieve perfect conductance, in general is in accord with the renormalization group (RG) viewpoint. For nonzero energy ϵ, particle-hole symmetry is broken so the scattering amplitude λ can be complex. In the special case $\epsilon = 0$ where particle-hole symmetry holds there is only one condition for perfect conductance $t'^2_\ell/t^2_\ell = t'^2_r/t^2_r$ and only one parameter needs to be adjusted.

Now let us consider the case with nontrivial t_i' within the narrow band approximation. We use the parametrization

$$\begin{aligned} t_\ell' &= t_\ell + \delta t_\ell' = t - \delta t + \delta t_\ell', \\ t_r' &= t_r + \delta t_r' = t + \delta t + \delta t_r' . \end{aligned} \tag{B3}$$

In this case, there is another backscattering perturbation term

$$\begin{aligned} \delta\hat{H}' = &-2\delta t_\ell' \psi_-^\dagger \psi_+ e^{-ik_F a} - 2\delta t_r' \psi_-^\dagger \psi_+ e^{ik_F a} + \text{H.c.} \\ &-(\delta t_\ell' + \delta t_r') 2\cos[k_F a](\psi_-^\dagger \psi_- + \psi_+^\dagger \psi_+), \end{aligned} \tag{B4}$$

where ψ_- and ψ_+ are evaluated at $x = 0$ in all terms. Focusing on the backscattering term the perturbation becomes

$$\delta\hat{H} + \delta\hat{H}' = 2\pi i \lambda \psi_-^\dagger \psi_+(x = 0) + \text{H.c.} \tag{B5}$$

with

$$\lambda = \frac{u_\ell - u_r}{4\pi a} + \frac{i\delta t_\ell' e^{-ik_F a} + i\delta t_r' e^{ik_F a}}{\pi} . \tag{B6}$$

Although the variations in t_i are small, they occur over only three sites, so this is not an adiabatic change. Note that while we were able to determine λ explicitly in this model, with all t_i nearly equal, it may not be feasible to do so in all cases. In fact, a reduction to a narrow band model is not accurate in general, as discussed in the main text.

2. Next-nearest-neighbor hopping

Next-nearest-neighbor hopping can also be added to the Hamiltonian, explicitly breaking particle-hole symmetry. We consider the Hamiltonian

$$\hat{H}_0' = \sum_i [-t_{1,j} \psi_i^\dagger \psi_{i+1} - t_{2,i} \psi_i^\dagger \psi_{i+2} + \text{H.c.}] . \tag{B7}$$

To keep things as simple as possible we choose

$$t_{1,i} = \begin{cases} t_{1L}, & (i \leqslant -1), \\ t_{1R}, & (i \geqslant 0), \end{cases} \qquad t_{2,i} = \begin{cases} t_{2L}, & (i \leqslant -2), \\ t_{2R}, & (i \geqslant 0). \end{cases} \tag{B8}$$

There is no particularly simple or natural choice for $t_{2,-1}$ so it is kept as a free parameter. Let us assume that all the $t_{1,i}$ are close together and all the $t_{2,i}$ are close together so that the narrow band approach is applicable. Thus we write

$$\begin{aligned} t_{1L} &= t_1 - \delta t_1 , \quad t_{2L} = t_2 - \delta t_2 , \\ t_{1R} &= t_1 + \delta t_1 , \quad t_{2R} = t_2 + \delta t_2 , \\ t_{2,-1} &= t_2 + \delta t . \end{aligned} \tag{B9}$$

A simple extension of the previous calculation gives

$$\pi\lambda = -\delta t_1 \csc[k_F a] - \delta t_2 \cot[k_F a] + i\delta t e^{2ik_F a} \tag{B10}$$

for the backscattering coupling constant.

As a simpler special case, consider $k_F = \pi/2$. Now

$$\pi\lambda = -\delta t_1 - \delta t_2 - i\delta t , \tag{B11}$$

and λ is complex in this case despite being at half-filling; this is natural since t_2 breaks particle-hole symmetry at all fillings.

APPENDIX C: BOSONIZATION DETAILS

First we note the following useful relations:

$$\begin{aligned} \psi_\alpha^\dagger(x)\psi_\alpha(x) &= \rho_\alpha(x) \equiv -\frac{1}{\sqrt{\pi}} \partial_x \phi_\alpha(x), \\ \psi_\alpha^\dagger(x)\partial_x\psi_\alpha(x) &= \alpha i \pi \rho_\alpha^2(x), \quad \text{and} \\ \psi_\alpha^\dagger(x)\psi_{-\alpha}(x) &= \frac{i\alpha}{2\pi a} e^{-i\alpha\sqrt{4\pi}\phi(x)}. \end{aligned} \tag{C1}$$

Due to the inhomogeneous nature of both the Fermi momentum and the interactions, the $2k_{F,x}$ oscillating terms in the interaction can no longer be neglected, see Eq. (3.5). One finds a nonzero contribution to the backscattering around any region of inhomogeneity. These terms must be treated carefully, as an example we can take $: \psi_\alpha^\dagger\psi_\alpha(x) :: \psi_\alpha^\dagger\psi_{-\alpha}(x+a) :$. Direct rearrangement gives for $\psi_\alpha^\dagger\psi_\alpha(x)\psi_\alpha^\dagger\psi_{-\alpha}(x+a)$ either

$$\begin{aligned} &: \psi_\alpha^\dagger\psi_\alpha(x) :: \psi_\alpha^\dagger\psi_{-\alpha}(x+a) : \\ &\quad + \langle 0|\psi_\alpha^\dagger\psi_\alpha(x)|0\rangle : \psi_\alpha^\dagger\psi_{-\alpha}(x+a) : \end{aligned} \tag{C2}$$

or

$$\begin{aligned} &- : \psi_\alpha^\dagger(x)\psi_{-\alpha}(x+a) :: \psi_\alpha^\dagger(x+a)\psi_\alpha(x) : \\ &- : \psi_\alpha^\dagger(x)\psi_{-\alpha}(x+a) : \langle 0|\psi_\alpha^\dagger(x+a)\psi_\alpha(x)|0\rangle , \end{aligned} \tag{C3}$$

which are therefore equal. Then, using

$$\langle 0|\psi_\alpha^\dagger(x+a)\psi_\alpha(x)|0\rangle \approx i\alpha/2\pi a , \tag{C4}$$

and expanding in the cutoff a this allows us to write

$$\begin{aligned} &: \psi_\alpha^\dagger\psi_\alpha(x) :: \psi_\alpha^\dagger\psi_{-\alpha}(x+a) \\ &\quad :\approx -\langle 0|\psi_\alpha^\dagger\psi_\alpha(x)|0\rangle : \psi_\alpha^\dagger\psi_{-\alpha}(x+a) : \\ &\qquad - : \psi_\alpha^\dagger(x)\psi_{-\alpha}(x+a) : \\ &\qquad \times \left(\frac{i\alpha}{2\pi a} + \rho_\alpha(x) + a\psi_\alpha^\dagger\partial_x\psi_\alpha(x) \right) . \end{aligned} \tag{C5}$$

Now keeping only the leading order terms we find

$$: \psi_\alpha^\dagger\psi_\alpha(x) :: \psi_\alpha^\dagger\psi_{-\alpha}(x+a) :\approx \frac{e^{-i\alpha\sqrt{4\pi}\phi(x)}}{4\pi^2 a^2} . \tag{C6}$$

Similar expressions hold for the other terms.

The bosonized free and interacting Hamiltonians become

$$\begin{aligned} \hat{H}_0 = &-\sum_{x\alpha} \alpha i t_x a^2 e^{i\alpha\kappa_x^-} (\partial_x\phi_\alpha)^2 + \text{H.c.} \\ &-\sum_{x\alpha} \frac{i\alpha t_x}{\pi} e^{-2i\alpha k_{F,x}x - i\alpha\sqrt{4\pi}\phi(x)} \left[e^{-i\alpha\kappa_x^-} + \frac{V}{2t_x} \right], \end{aligned} \tag{C7}$$

and

$$\begin{aligned} \hat{H}_I = \sum_{x\alpha} a^2 U_x \Bigg[&(1 - e^{-2i\alpha\kappa_x^-}) \frac{(\partial_x\phi)^2}{2\pi} \\ &+ e^{2i\alpha k_{F,x}x} (e^{2i\alpha\kappa_x^-} - 1) \frac{2e^{i\alpha\sqrt{4\pi}\phi(x)}}{(2\pi a)^2} \\ &- e^{4i\alpha\kappa_x^+} \frac{e^{i\alpha 2\sqrt{4\pi}\phi(x)}}{(2\pi a)^2} \Bigg], \end{aligned} \tag{C8}$$

respectively. Included in this is the irrelevant umklapp scattering

$$\hat{H}_U = -\sum_x a \frac{U_x}{\pi^2 a} \cos[4\kappa_x^+ + 2\sqrt{4\pi}\phi(x)]\,. \tag{C9}$$

Away from half-filling this is only a boundary contribution.

APPENDIX D: GREEN'S FUNCTION AND RENORMALIZATION GROUP CALCULATIONS

For the abrupt jump of Sec. III A the Green's function, at $\lambda = 0$, can be calculated exactly. We have

$$\begin{aligned} &G(x,y;\tau) = T\sum_m e^{i\omega_m \tau} G_m(x,y) \quad \text{and} \\ &\left[\frac{\omega_m^2}{2g_x u_x} - \frac{\partial}{\partial x}\left(\frac{u_x}{2g_x}\frac{\partial}{\partial x}\right)\right] G_m(x,y) = \delta(x-y)\,. \end{aligned} \tag{D1}$$

Solving this differential equation subject to the appropriate boundary conditions [17,27] gives

$$\begin{aligned} G(x,y;\tau) &= \langle \phi(x,0)\phi(y,\tau)\rangle \\ &= -\frac{\bar{g}}{\pi}\ln\left|\sinh\left[\pi T\left(\frac{|x|}{u_x}+\frac{|y|}{u_y}-i\tau\right)\right]\right| \\ &\quad + \frac{\mathcal{L}[x,y]g_x}{\pi}\ln\left|\frac{\sinh\left[\pi T\left(\frac{|x|}{u_x}+\frac{|y|}{u_y}-i\tau\right)\right]}{\sinh\left[\pi T\left(\frac{|x-y|}{u_x}-i\tau\right)\right]}\right|. \end{aligned} \tag{D2}$$

We have introduced $2\mathcal{L}[x,y] \equiv 1 + \mathrm{sgn}[x]\,\mathrm{sgn}[y]$.

The renormalization procedure is done in the standard manner by expanding the perturbation, $\exp(-\int d\tau H')$, to first order and integrating out the fields with fast Fourier components near the band edge $\Lambda' < |k| < \Lambda$. To recover the original form after re-exponentiating the action we rescale $\Lambda\tau_{\text{new}} = \Lambda'\tau$, and define the new coupling constant λ, as

$$\lambda(\Lambda') = \frac{\Lambda}{\Lambda'}\lambda(\Lambda)e^{-\pi\tilde{G}_>(x=y=\tau=0)}\,, \tag{D3}$$

where $\tilde{G}_>$ is the Green's function after integrating out the fast modes.

Therefore for the RG equation what we need is the Green's function summed over the fast modes. First let us change variables to $r = x - y$ and $R = (x+y)/2$. Then, with $u(r, R=0) = 2u_x u_y/(u_x+u_y)|_{x=-y} = 2u_\ell u_r/(u_\ell+u_r) \equiv u$, we have

$$G(r, R=0;\tau) = -\frac{\bar{g}}{\pi}\ln\left|\sinh\left[\pi T\left(\frac{|r|}{u}-i\tau\right)\right]\right|. \tag{D4}$$

This is the same as the Green's function for a homogeneous case, but with a new velocity and a new Luttinger parameter

$$\frac{1}{\bar{g}} = \frac{1}{2}\left[\frac{1}{g_\ell}+\frac{1}{g_r}\right]. \tag{D5}$$

Now we require

$$\begin{aligned} G_>(0,0;0) &= \sum_{\Lambda'<|k|<\Lambda} G(k, R=\tau=0) \\ &= \sum_{\Lambda'<|k|<\Lambda}\int dr e^{ikr} G(r, R=\tau=0)\,. \end{aligned} \tag{D6}$$

Thus integrating out the fast Fourier components results in a change of the Green's function

$$G_> \approx \frac{\bar{g}}{\pi} d\ln\Lambda\,, \tag{D7}$$

which governs the renormalization in the usual manner:

$$\frac{1}{\lambda}\frac{d\lambda}{d\ln\Lambda} = 1 - \bar{g}\,. \tag{D8}$$

We therefore expect that the effective backscattering renormalizes as a power law in the temperature $R \propto T^{\bar{g}-1}$, which in turn affects the conductance and other physical observables accordingly. This has been confirmed numerically [27].

APPENDIX E: USEFUL SUMS FOR THE BOUNDARY TERMS

To find the coefficients of the backscattering terms several sums are needed. We want

$$I \equiv \sum_{\substack{x=ja\\ j\in\mathbb{Z}}} e^{-2ik_{F,x}x} F(x) O(x) \tag{E1}$$

in the particular case where we can write

$$F(x) = \underbrace{F_\ell\,\Theta(-x-a)}_{\equiv F_\ell(x)} + \underbrace{F_r\,\Theta(x)}_{\equiv F_r(x)} \tag{E2}$$

with $\Theta(0) \equiv 1$. Assuming O_x is slowly varying on a length scale of a, this allows us to write

$$\begin{aligned} I &\approx O(x=0) \sum_{\substack{x=ja\\ j\in\mathbb{Z}}} \sum_{i=1,2} e^{-2ik_{Fi}x} F_i(x) \\ &\approx O(x=0) \sum_{\substack{x=ja\\ j\in\mathbb{Z}}} \sum_{i=1,2} e^{-2ik_{Fi}x} \frac{\mathcal{Z}_i}{2}[F_i(x) - F_i(x+a)]\,, \end{aligned} \tag{E3}$$

with $\mathcal{Z}_i = 1 + i\cot[k_{Fi}a]$. Only a single term of each sum over x is nonzero and we find

$$I \approx O(x=0)\left[\frac{iF_\ell e^{ik_{F\ell}a}}{2\sin[k_{F\ell}a]} - \frac{iF_r e^{ik_{Fr}a}}{2\sin[k_{Fr}a]}\right]. \tag{E4}$$

We may also be interested in the case where

$$F(x) = \underbrace{F_\ell\,\Theta(-x-a)}_{\equiv F_\ell(x)} + \underbrace{F_r\,\Theta(x-a)}_{\equiv F_r(x)} + F_0\delta(x) \tag{E5}$$

and we can independently change F_0 on the central site. Then with $I \approx O_{x=0}\lambda$ we find

$$\lambda = F_0 + \frac{iF_\ell e^{ik_{F\ell}a}}{2\sin[k_{F\ell}a]} - \frac{iF_r e^{-ik_{Fr}a}}{2\sin[k_{Fr}a]}\,. \tag{E6}$$

APPENDIX F: MODE EXPANSION AND ITS CORRELATION FUNCTIONS

Let us first consider the solutions of the classical equation of motion, Eq. (4.3), subject to the boundary conditions Eq. (4.5). There are two types of oscillating solutions

$$\phi_k^{(1)}(x,t) \sim e^{ikt}\cos(kx) \tag{F1}$$

with $\partial_x\phi(x=0)=0$, and

$$\phi_k^{(2)} \sim g_x e^{ikt}\sin(kx) \tag{F2}$$

with $\phi(x=0)=0$. In addition there are solutions linear in x and t. The solutions linear in x have the form

$$\phi^x(x,t) \sim g_x x\,. \tag{F3}$$

The bosonization formula (3.6) implies that the bosonic field ϕ is periodic with period $\phi+\sqrt{\pi}$. Furthermore we are considering solutions on a ring with circumference $2L$ thus $\phi(x)=\phi(x+2L)+\sqrt{\pi}n$. The oscillatory solutions of both types therefore must have $k=\pi l/L$ for $l=1,2,3,\ldots$. For the solutions linear in x the same periodicity conditions imply

$$\phi^x(x,t) = \frac{\sqrt{\pi}n}{2\bar{\gamma}L}x g_x\,. \tag{F4}$$

Let us now consider the mode expansion. $\hat{\Pi}$ is canonically conjugate to ϕ_0 and the normalization of each term is fixed by requiring the canonical commutation relations to hold. For $g_\ell \neq g_r$, we may expand in solutions of the classical equations of motion, while respecting the canonical commutation relations. This leads to the mode expansion given in Eq. (4.7).

Using the mode expansion we can first calculate the bosonic commutators in the ground state. We find that

$$\begin{aligned}\mathrm{Re}\langle\tilde{\phi}(x,t)\tilde{\phi}(x,0)\rangle = &-\frac{1}{\bar{\gamma}}\frac{1}{8\pi}\ln\left|2^4\sin[\pi(t-2x)/2L]\sin[\pi(t+2x)/2L]\sin^2[\pi t/2L]\right| \\ &+\frac{\bar{g}}{g_x^2}\frac{1}{8\pi}\ln\left|\frac{\sin[\pi(t-2x)/2L]\sin[\pi(t+2x)/2L]}{\sin^2[\pi t/2L]}\right|\end{aligned} \tag{F5}$$

and

$$\begin{aligned}\mathrm{Re}\langle\phi(x,t)\phi(x,0)\rangle = &-\frac{\bar{g}}{8\pi}\ln\left|2^4\sin[\pi(t-2x)/2L]\sin[\pi(t+2x)/2L]\sin^2[\pi t/2L]\right| \\ &+\frac{g_x^2}{\bar{\gamma}}\frac{1}{8\pi}\ln\left|\frac{\sin[\pi(t-2x)/2L]\sin[\pi(t+2x)/2L]}{\sin^2[\pi t/2L]}\right|.\end{aligned} \tag{F6}$$

Finally

$$\mathrm{Re}\left\langle\tilde{\phi}(x,t)\phi(x,0)\right\rangle = \frac{1}{8\pi}\left[\frac{g_x}{\bar{\gamma}}+\frac{\bar{g}}{g_x}\right]\ln\left|\frac{\sin[\pi(t-2x)/2L]}{\sin[\pi(t+2x)/2L]}\right| \tag{F7}$$

is also useful.

[1] W. Liang, M. Bockrath, D. Bozovic, J. Hafner, M. Tinkham, and H. Park, Nature (London) **411**, 665 (2001).
[2] A. Javey, J. Guo, Q. Wang, M. Lundstrom, and H. Dai, Nature (London) **424**, 654 (2003).
[3] A. Yacoby, H. L. Stormer, N. S. Wingreen, L. N. Pfeiffer, K. W. Baldwin, and K. W. West, Phys. Rev. Lett. **77**, 4612 (1996).
[4] H. Steinberg, G. Barak, A. Yacoby, L. N. Pfeiffer, K. W. West, B. I. Halperin, and K. L. Hur, Nat. Phys. **4**, 116 (2008).
[5] S. Tarucha, T. Honda, and T. Saku, Solid State Commun. **94**, 413 (1995).
[6] S. Tomonaga, Prog. Theor. Phys. **5**, 544 (1950).
[7] J. M. Luttinger, J. Math. Phys. **4**, 1154 (1963).
[8] T. Giamarchi, *Quantum Physics in One Dimension* (Clarendon, Oxford, 2004).
[9] C. L. Kane and M. P. A. Fisher, Phys. Rev. B **46**, 15233 (1992).
[10] C. L. Kane and M. P. A. Fisher, Phys. Rev. Lett. **68**, 1220 (1992).
[11] S. Eggert and I. Affleck, Phys. Rev. B **46**, 10866 (1992).
[12] A. Furusaki and N. Nagaosa, Phys. Rev. B **47**, 4631 (1993).
[13] R. G. Pereira and E. Miranda, Phys. Rev. B **69**, 140402 (2004).
[14] N. Sedlmayr, S. Eggert, and J. Sirker, Phys. Rev. B **84**, 024424 (2011).
[15] D. Yue, L. I. Glazman, and K. A. Matveev, Phys. Rev. B **49**, 1966 (1994).
[16] I. Safi and H. J. Schulz, Phys. Rev. B **52**, R17040 (1995).
[17] D. L. Maslov and M. Stone, Phys. Rev. B **52**, R5539 (1995).
[18] M. Ogata and H. Fukuyama, Phys. Rev. Lett. **73**, 468 (1994).
[19] E. Wong and I. Affleck, Nucl. Phys. B **417**, 403 (1994).
[20] C. C. Chamon and E. Fradkin, Phys. Rev. B **56**, 2012 (1997).
[21] K. I. Imura, K. V. Pham, P. Lederer, and F. Piéchon, Phys. Rev. B **66**, 035313 (2002).
[22] T. Enss, V. Meden, S. Andergassen, X. Barnabe-Theriault, W. Metzner, and K. Schönhammer, Phys. Rev. B **71**, 155401 (2005); K. Janzen, V. Meden, and K. Schönhammer, *ibid.* **74**, 085301 (2006).
[23] J. Rech and K. A. Matveev, J. Phys.: Condens. Matter **20**, 164211 (2008).
[24] J. Rech and K. A. Matveev, Phys. Rev. Lett. **100**, 066407 (2008).

[25] D. B. Gutman, Y. Gefen, and A. D. Mirlin, Phys. Rev. B **81**, 085436 (2010).
[26] R. Thomale and A. Seidel, Phys. Rev. B **83**, 115330 (2011).
[27] N. Sedlmayr, J. Ohst, I. Affleck, J. Sirker, and S. Eggert, Phys. Rev. B **86**, 121302 (2012).
[28] N. Sedlmayr, P. Adam, and J. Sirker, Phys. Rev. B **87**, 035439 (2013).
[29] I. Safi and H. J. Schulz, Phys. Rev. B **59**, 3040 (1999).
[30] A. Furusaki and N. Nagaosa, Phys. Rev. B **54**, R5239 (1996).
[31] F. D. M. Haldane, Phys. Rev. Lett. **47**, 1840 (1981).
[32] F. D. M. Haldane, J. Phys. C **14**, 2585 (1981).
[33] J. Friedel, Il Nuovo Cimento **7**, 287 (1958).
[34] R. Egger and H. Grabert, Phys. Rev. Lett. **75**, 3505 (1995).
[35] S. Eggert and I. Affleck, Phys. Rev. Lett. **75**, 934 (1995).
[36] S. A. Söffing, M. Bortz, I. Schneider, A. Struck, M. Fleischhauer, and S. Eggert, Phys. Rev. B **79**, 195114 (2009).
[37] S. Rommer and S. Eggert, Phys. Rev. B **62**, 4370 (2000).
[38] O. F. Syljuåsen and A. W. Sandvik, Phys. Rev. E **66**, 046701 (2002).
[39] A. Dorneich and M. Troyer, Phys. Rev. E **64**, 066701 (2001).
[40] M. Takahashi, *Thermodynamics of One-Dimensional Solvable Problems* (Cambridge University Press, Cambridge, England, 1999).
[41] F. H. L. Essler, H. Frahm, F. Göhmann, A. Klümper and V. E. Korepin, *The One-Dimensional Hubbard Model* (Cambridge University Press, Cambridge, England, 2005).
[42] R. G. Pereira, J. Sirker, J.-S. Caux, R. Hagemans, J. M. Maillet, S. R. White, and I. Affleck, J. Stat. Mech. (2007) P08022.
[43] J. Sirker, Int. J. Mod. Phys. B **26**, 1244009 (2012).
[44] C. Blumenstein, J. Schäfer, S. Mietke, S. Meyer, A. Dollinger, M. Lochner, X. Y. Cui, L. Patthey, R. Matzdorf, and R. Claessen, Nat. Phys. **7**, 776 (2011).
[45] S. Eggert, H. Johannesson, and A. Mattsson, Phys. Rev. Lett. **76**, 1505 (1996).
[46] S. Eggert, Phys. Rev. Lett. **84**, 4413 (2000).
[47] P. Kakashvili, H. Johannesson, and S. Eggert, Phys. Rev. B **74**, 085114 (2006).
[48] F. Anfuso and S. Eggert, Phys. Rev. B **68**, 241301(R) (2003).
[49] I. Schneider and S. Eggert, Phys. Rev. Lett. **104**, 036402 (2010).
[50] S. A. Söffing, I. Schneider, and S. Eggert, Europhys. Lett. **101**, 56006 (2013).
[51] I. Affleck and A. W. W. Ludwig, Phys. Rev. Lett. **67**, 161 (1991).
[52] R. Landauer, IBM J. Res. Dev. **1**, 223 (1957).